Am J Physiol Endocrinol Metab 283: E383–E389, 2002.
First published April 23, 2002; 10.1152/ajpendo.00547.2001.

Temporal gradients in shear stimulate osteoblastic proliferation via ERK1/2 and retinoblastoma protein

GUANG-LIANG JIANG,* CHARLES R. WHITE,* HAZEL Y. STEVENS, AND JOHN A. FRANGOS
Department of Bioengineering, University of California, San Diego, La Jolla, California 92093

Received 12 December 2001; accepted in final form 9 April 2002

Jiang, Guang-Liang, Charles R. White, Hazel Y. Stevens, and John A. Frangos. Temporal gradients in shear stimulate osteoblastic proliferation via ERK1/2 and retinoblastoma protein. *Am J Physiol Endocrinol Metab* 283: E383–E389, 2002. First published April 23, 2002; 10.1152/ajpendo.00547.2001.—Bone cells are subject to interstitial fluid flow (IFF) driven by venous pressure and mechanical loading. Rapid dynamic changes in mechanical loading cause transient gradients in IFF. The effects of pulsatile flow (temporal gradients in fluid shear) on rat UMR106 cells and rat primary osteoblastic cells were studied. Pulsatile flow induced a 95% increase in S-phase UMR106 cells compared with static controls. In contrast, ramped steady flow stimulated only a 3% increase. Similar patterns of S-phase induction were also observed in rat primary osteoblastic cells. Pulsatile flow significantly increased relative UMR106 cell number by 37 and 62% at 1.5 and 24 h, respectively. Pulsatile flow also significantly increased extracellular signal-regulated kinase (ERK1/2) phosphorylation by 418%, whereas ramped steady flow reduced ERK1/2 activation to 17% of control. Correspondingly, retinoblastoma protein was significantly phosphorylated by pulsatile fluid flow. Inhibition of mitogen-activated protein (MAP)/ERK kinase (MEK)1/2 by U0126 (a specific MEK1/2 inhibitor) reduced shear-induced ERK1/2 phosphorylation and cell proliferation. These findings suggest that temporal gradients in fluid shear stress are potent stimuli of bone cell proliferation.

shear stress; pulsatile fluid flow; osteoblasts

(RE)MODELING OF BONE in the skeletal system is strongly influenced by mechanical loading and unloading. Exercise has been shown to stimulate increases in bone mass (24), whereas prolonged mechanical unloading results in bone atrophy (36, 45). It has been hypothesized that exercise-induced (re)modeling of bone may result from stimulation of osteoblasts by interstitial fluid flow (IFF) through the porous structure of bone (10, 31). Interstitial fluid flows radially outward through the bone cortex and is driven by hydrostatic pressure gradients across the cortex and pressure gradients from mechanical loading (21, 23, 39, 42). Theoretical models of IFF indicate significant fluid shear stresses in the canaliculi ranging between 6 and 30 dyn/cm^2 (44). During physical activity, rapid dynamic changes in mechanical loading cause transient changes in bone marrow pressure and IFF (30, 43). Rapid changes in IFF subject bone cells to large temporal gradients in interstitial fluid shear stress. Temporal shear stress gradients are defined as the rapid change in shear stress over a small period of time ($<$0.5 s) at any given location on the cell surface. Steady shear stress is devoid of temporal gradients and can be established if the onset and/or cessation of flow is slowly transitioned. In any given system of flow, if the change in flow is sudden, significant temporal gradients are generated (8, 46). Given that similar temporal gradients in shear stress in other cell types have been shown to be promitogenic compared with steady fluid flow (2), repeated temporal gradients in shear stress through the bone matrix may also stimulate osteoblast proliferation (10, 43).

A number of investigators have demonstrated that IFF stimulates elaborate mechanochemical signaling cascades in osteoblasts. Fluid shear has been shown to stimulate osteoblast production and release of cAMP, prostaglandin E_2 (PGE_2), inositol triphosphate, and nitric oxide (NO) (17, 32–34). Osteoblasts respond not only to steady IFF but also to shear intensity and frequency of fluid flow (11, 16, 22). Pulsatile flow has been shown to stimulate greater PGE_2 production in osteoblasts compared with steady flow (31). The activation of G proteins is essential for the flow-mediated responses in osteoblasts (32). Temporal gradients in shear cause a fourfold higher NO release, which is mediated by a G protein- and calcium-dependent pathway. In contrast, steady fluid flow devoid of temporal gradients stimulates a low level of NO release, which is independent of the G protein and calcium pathway (22). Although IFF mediates both local and systemic bone homeostasis by stimulating the release of autocrine/paracrine factors that alter the dynamic balance between osteoblast and osteoclast activity, the cellular response and signaling pathways that dictate osteoblast proliferation are poorly understood. The promitogenic effect of IFF may be mediated via a mitogen-activated protein kinase (MAPK) pathway. MAPKs are members of a conserved cascade of kinases that stimulate phosphorylation of transcription factors and other targets in response to extracellular signals such

*These authors contributed equally to the writing of this study.

Address for reprint requests and other correspondence: J. A. Frangos, Dept. of Bioengineering, Univ. of California, San Diego, La Jolla, CA 92093-0412 (E-mail: frangos@ucsd.edu).

The costs of publication of this article were defrayed in part by the payment of page charges. The article must therefore be hereby marked "*advertisement*" in accordance with 18 U.S.C. Section 1734 solely to indicate this fact.

as growth factors, cytokines, and fluid shear stress (47). In higher eukaryotes, the physiological role of MAPK signaling has been correlated with cellular events such as proliferation and progression of the cell cycle (4, 15). In endothelial cells, fluid shear stress has been demonstrated to rapidly activate a specific member of the MAPK family, extracellular signal-regulated kinase (ERK1/2) (2). The ERK pathway is thought to be involved primarily in the regulation of cell proliferation and differentiation (19), whereas other members of the MAPK family, such as stress-activated protein kinase/c-Jun-NH_2-terminal kinase and p38, may also be important in the regulation of cell apoptosis and inflammation (12, 18, 26). ERK1/2 is believed to mediate cell proliferation through the phosphorylation of other downstream proteins, one of which is retinoblastoma protein (Rb), which controls the cell cycle transition from G1 phase to S phase (19, 37).

To better elucidate the underlying shear-induced signal transduction pathway, the present studies examined the effect of repeated temporal gradients (pulsatile fluid flow) and ramped steady flow devoid of temporal gradients on rat osteoblast-like sarcoma cell (UMR106) and rat primary osteoblastic cell proliferation. The shear-induced activation of the ERK1/2-signaling pathway and the regulation of cell cycle progression via Rb phosphorylation was investigated.

MATERIALS AND METHODS

Cell culture and treatment. Rat osteosarcoma UMR106 cells were seeded onto collagen-coated glass microscope slides at 5×10^5 cells per slide. Cells were grown to confluence within 72 h in DMEM (Irvine Scientific). Medium was supplemented with 2% FBS (Biocell), 0.5 U/ml penicillin, and 0.05 mg/ml streptomycin. Confluent cell cultures used for the ERK1/2 inhibition assay were pretreated with 30 μM U0126 (a specific inhibitor of the MAPK/ERK kinase (MEK)1/2 enzyme; Calbiochem) or vehicle for 1 h (27). All cell cultures were maintained in a humidified 5% CO_2-95% air incubator at 37°C.

Isolation and characterization of rat primary osteoblasts were prepared using techniques previously described (25, 40). Briefly, femora collected from 3-wk-old female rats were dissected free of epiphysial cartilage, cleaned of marrow, and minced finely. Chips were incubated in trypsin (2.5 mg/ml) at 37°C for 10 min, washed and then incubated in collagenase type IV (Sigma; 1 mg/ml) in Hanks' balanced salt solution for 1 h at 37°C. Cells were resuspended in α-MEM containing 10% FCS and plated. At confluence, the cells were trypsinized (*day 0, batch 1*) and plated at 4.5×10^3 cells/cm^2 in α-MEM and 10% FCS with medium changed every 2nd day. At confluence, cells were supplemented with 100 μg/ml ascorbic acid and 10 mM β-glycerophosphate to promote differentiation, and medium was changed every 2nd day. The cultures were maintained for 16 days of supplementation (*batch 2*) and analyzed for expression of osteoblastic features. Cells were fixed in 4% paraformaldehyde for alkaline phosphatase activity (41) and in 70% ethanol for alizarin red detection of bone nodules (38). Primary osteoblastic cells supplemented with mineralization medium produced bone nodules (*day 16*) and were heterogeneous with patchy staining for alkaline phosphatase activity.

Flow experiments. Protein-free DMEM supplemented with 0.5 U/ml penicillin and 0.05 mg/ml streptomycin was used as the perfusing medium for all experimental procedures. Medium perfusion was driven by a computer-controlled syringe pump through a conventional parallel-plate flow chamber (2). All flow chambers and accompanying apparatus were maintained at 37°C throughout the experiment. Time-matched sham controls, where cells were placed on the chamber without perfusion, were performed for all experimental groups.

Confluent UMR106 monolayers and rat primary osteoblastic cells were subjected to one of the following laminar flow files. *1*) Ramped steady flow (a smooth 30-s ramped increase from 0 to 12 dyn/cm^2, sustained steady shear for 7 min, and a smooth 30-s ramped decrease). Cells were left on the chamber for an additional 7 min after the cessation of flow. *2*) One-hertz pulsatile (a repeated sequence of square-wave impulses of 12 dyn/cm^2 at a frequency of 1 Hz for 15 min). *3*) Cells were removed immediately after the cessation of flow. Both profiles exposed cells to the same total volume of perfusion medium (100 ml) over 15 min.

Cell proliferation assay. Proliferating UMR106 cells and rat primary osteoblastic cells were identified by using a commercially available in situ monoclonal antibody kit for the detection of bromodeoxyuridine (BrdU) incorporation into cellular DNA during cell division (Boehringer Mannheim). Immediately after exposure to flow, slides were removed from the chamber and allowed to recover in an incubator at 37°C for 1 h before the addition of BrdU. UMR106 cells were labeled with 10 mM BrdU for 30 min. Rat primary osteoblastic cells were labeled with 10 mM BrdU for 30 min or 24 h. Slides were then fixed with 70% ethanol (in 50 mM glycine buffer, pH 2.0) and immunostained for BrdU incorporation. To identify all cell nuclei, slides were double stained with 4,6-diamidino-2-phenylindole (DAPI). BrdU- and DAPI-positive cells were visualized under a fluorescence microscope (Nikon, Diaphot TMD). Six random, nonoverlapping, ×40 high-power fields of view were photographed. DAPI-positive and corresponding BrdU-positive cells were visually counted.

Total cell numbers were also independently assessed from parallel cultures. Cells were trypsinized and counted by the trypan blue exclusion assay.

Western blot analysis. Cells were collected at 30, 60, and 90 min after fluid flow stimulation. Cells were quickly washed with ice-cold PBS and lysed in buffer (50 mM HEPES, pH 7.4, 250 mM NaCl, 0.1% Nonidet P-40, 1 mM dithiothreitol, and 1 mM EDTA) at 4°C for 30 min. Samples were clarified by centrifugation, and protein concentrations were determined. Proteins were resolved by 12% SDS-PAGE for ERK1/2 activation and 4–20% gradient SDS-PAGE for Rb. Proteins were subsequently electroblotted onto Immobilon-P membranes (Millipore). Membranes were blocked with 4% nonfat milk in 50 mM Tris·HCl, 150 mM NaCl, and 0.1% Tween 20 buffer (pH 8.0). Membranes were agitated in the same buffer with primary antibodies overnight at 4°C. Rabbit anti-ERK1/2, anti-phospho-(p)ERK1/2, and rabbit anti-pRb-780 were purchased from Cell Signaling Technology. Rabbit anti-Rb (c-15) was purchased from Santa Cruz Biotechnology; horseradish peroxidase-conjugated anti-rabbit was used as a secondary antibody (Cell Signaling). Immunodetection was carried out using enhanced chemiluminescence (Pierce). Protein band quantitation was performed on a DuoScan T2500 (AGFA).

Statistics. All experimental values are given as means ± SD. All reported values of n represent three separate experiments. Significant differences between means were calculated using a Student's t-test and ANOVA. Statistical significance was taken at the $P < 0.05$ level.

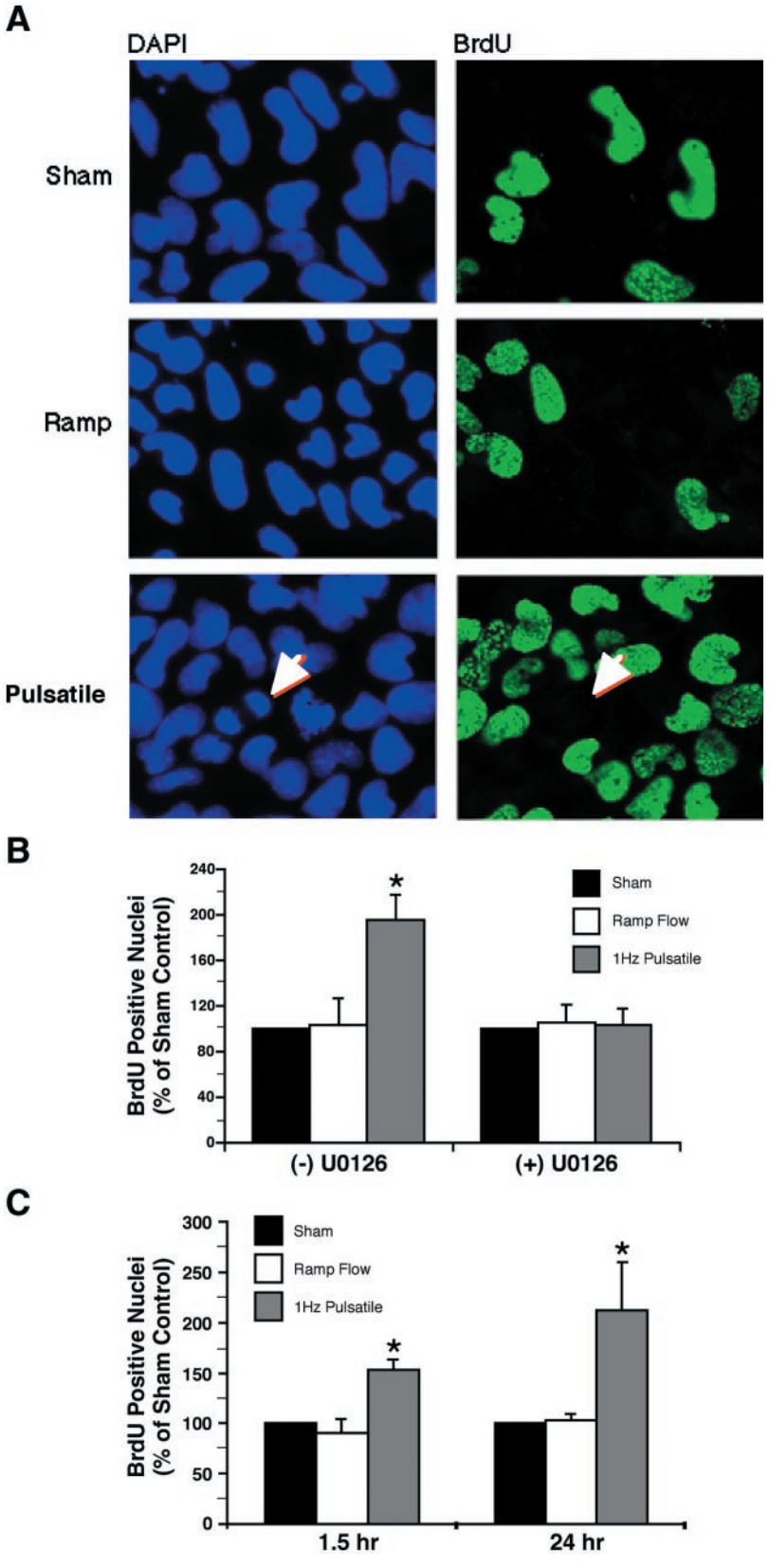

Fig. 1. Temporal gradients in shear, but not ramped steady flow, promoted DNA synthesis in UMR106 and primary rat osteoblastic cells. One hour after exposure to flow, cells were labeled with 10 mM bromodeoxyuridine (BrdU) for 30 min and immunostained for BrdU incorporation. *A*: typical nuclear 4,6-diamidino-2-phenylindole (DAPI; blue) and BrdU (green) immunostaining in UMR106 cells. Arrows indicate a telophase cell that had completed DNA synthesis before BrdU labeling. *B*: BrdU-positive UMR106 nuclei expressed as percent sham control. *Left*: BrdU incorporation in untreated cells 1 h after exposure to flow. *Right*: inhibition of extracellular signal-regulated kinase (ERK1/2) activity abolished flow-induced BrdU incorporation in U0126-treated cells 1 h after exposure to flow. *C*: BrdU-positive primary rat osteoblastic nuclei expressed as percent sham control at 1.5 h (*left*) and 24 h (*right*) after exposure to flow. Values are expressed as means ± SD. *Significant increase in BrdU labeling compared with both sham controls and ramped steady flow ($P < 0.002$, $n = 3$).

RESULTS

Effect of pulsatile and ramped steady flow on UMR106 and primary osteoblastic proliferation. In UMR106 cells, pulsatile fluid flow induced a 95 ± 22% mean increase in BrdU-positive cells compared with sham static controls ($P < 0.001$). In contrast, ramped steady flow stimulated no significant increase in BrdU uptake relative to sham static controls (3 ± 3%; Fig. 1, *A* and *B*). Furthermore, pulsatile flow significantly increased UMR106 cell number by 37 ± 24 and 62 ± 23% at 1.5 and 24 h after flow cessation, respectively ($P < 0.05$). Ramped steady flow had no effect on cell number (Fig. 2).

In primary osteoblastic cells, pulsatile fluid flow induced a significant 52 ± 10 and 111 ± 48% increase in BrdU-labeled cells relative to sham controls at 1.5 and 24 h after flow cessation, respectively ($P < 0.002$; Fig. 1*C*). In contrast, time-matched BrdU incorporation into primary osteoblastic cells exposed to ramped steady flow was not significantly different from that of time-matched sham controls (91 ± 12 and 104 ± 5%, 1.5 and 24 h, respectively).

Effect of pulsatile and ramped steady flow on the ERK1/2-signaling pathway and regulation of cell cycle. Pulsatile fluid flow resulted in a significant 14-fold increase in Rb phosphorylation relative to sham control ($P < 0.05$). Ramped steady flow induced only a fourfold increase in Rb phosphorylation (Fig. 3). To test whether pulsatile fluid flow-induced phosphorylation of Rb was mediated by a mitogen-activated protein kinase (MAPK) pathway, activation of ERK1/2 was monitored. Pulsatile fluid flow generated a significant fourfold peak increase in ERK1/2 phosphorylation (relative to sham controls) 30 min after the cessation of flow ($P < 0.05$; Fig. 4, *A* and *B*). Elevated levels of ERK1/2 phosphorylation were sustained over 90 min, whereas ramped steady flow did not significantly increase ERK1/2 phosphorylation over the same period. In contrast, ramped steady flow decreased ERK1/2

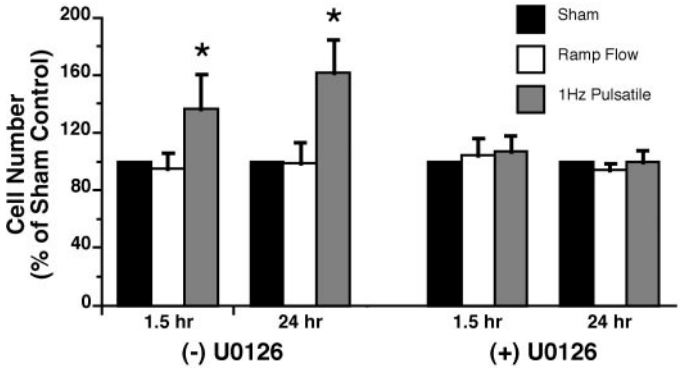

Fig. 2. Temporal gradients in shear, but not ramped steady flow, stimulated the proliferation of UMR106 cells. *Left*: in untreated cells, total cell number increased significantly relative to sham control 1.5 and 24 h after exposure to pulsatile fluid flow. *Right*: inhibition of ERK1/2 activity abolished flow-induced proliferation in U0126-treated cells 1.5 and 24 h after exposure to flow. Values are expressed as means ± SD. *Significant increase in cell number compared with both sham controls and ramped steady flow ($P < 0.05$, $n = 3$).

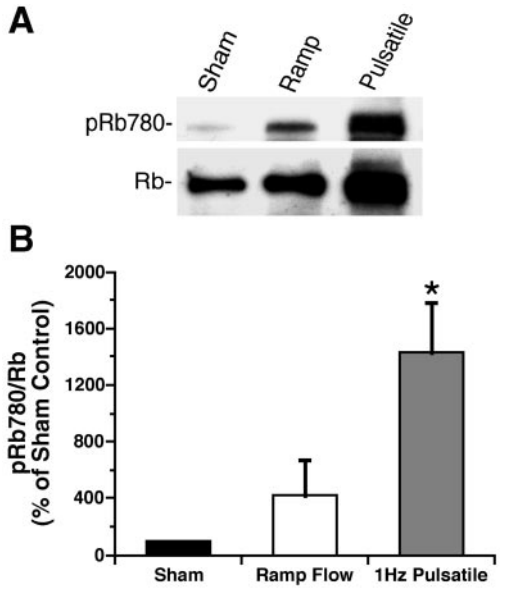

Fig. 3. Temporal gradients in shear stimulated the phosphorylation of retinoblastoma (Rb) protein. Rb samples were prepared 1.5 h after exposure to fluid flow. Equal amounts of total protein were resolved in SDS-PAGE. *A*: total Rb protein was probed with Rb c-15 antibody binding with both phosphorylated (p) and dephosphorylated forms. pRb was probed with pRb780 phosphorylation-specific antibody. *B*: densitometric quantification of Rb phosphorylation. Relative levels of pRb over Rb were obtained by dividing the levels of pRb/Rb in cells exposed to ramped steady flow or pulsatile flow by that in time-matched sham control cells. Values are expressed as means ± SD. *Significant increase in Rb phosphorylation compared with both sham controls and ramped steady flow ($P < 0.05$, $n = 3$).

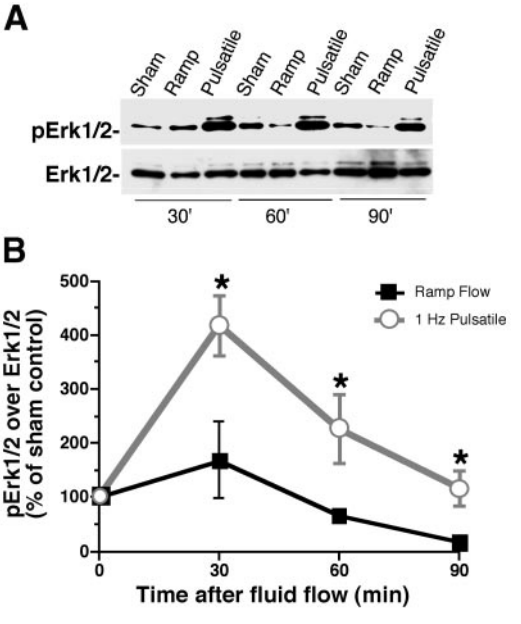

Fig. 4. Temporal gradients in shear, but not ramped steady flow, induced specific phosphorylation of ERK1/2. *A*: Western blot result showing both phosphorylated and total ERK1/2 proteins recognized by specific antibodies. *B*: densitometric quantification of flow-induced activation of ERK1/2. Relative levels of pERK1/2 over ERK1/2 were obtained by dividing the levels of pERK/ERK in cells exposed to ramped steady flow or pulsatile flow by that in time-matched sham control cells. Values are expressed as means ± SD. *Significant increase in ERK1/2 phosphorylation compared with ramped steady flow ($P < 0.001$, $n = 3$).

phosphorylation to 17% of control 90 min after the cessation of flow. Activation of ERK1/2 by fluid shear was inhibited with the addition of U0126 (Fig. 5*A*). Flow-induced phosphorylation of Rb was also inhibited when cells were treated with the MEK1/2 inhibitor U0126 (Fig. 5*B*).

To address whether inactivation of the MEK/ERK signal cascade can functionally affect shear-stimulated proliferation, BrdU incorporation was also assessed in the presence of U0126. U0126 treatment clearly abolished pulsatile fluid flow-stimulated proliferation (Figs. 1*B* and 2).

DISCUSSION

Exercise has long been recognized as a potent stimulant of bone (re)modeling (24). It has been hypothesized that exercise-induced remodeling of bone may result from stimulation of osteoblasts by IFF (10, 34). At rest, IFF is relatively steady, with only minor fluctuations driven by microvascular pressure pulsations (28). During physical activity, rapid dynamic changes in mechanical loading cause large temporal gradients in interstitial fluid shear stress induced by increases in intramedullary pressure (30, 43). Similar to other cell types (2, 46), osteoblasts selectively discriminate between distinct fluid flow profiles. Two distinct fluid flow profiles, steady shear stress and temporal gradients in shear, have been shown to stimulate different biochemical pathways in osteoblasts (16, 22). The present study is the first to demonstrate that temporal gradients in shear stimulate osteoblast proliferation. By use of well defined computer-controlled fluid flow profiles, repeated temporal gradients in shear stress (pulsatile fluid flow) were found to selectively promote the proliferation of cultured rat osteosarcoma UMR106 cells and primary rat osteoblastic cells. Conversely, steady shear stress devoid of temporal gradients (ramped steady flow) did not induce such a response. Furthermore, pulsatile fluid flow was shown to stimulate the progression of the cell cycle via the ERK1/2-signaling pathway and the subsequent phosphorylation of retinoblastoma protein.

In vivo, IFF has been associated with other biophysical phenomena, such as chemotransport and streaming potentials. Fluid flow increases chemotransport, generates a streaming potential, and subjects the endosteal surface and osteocytes in the canaliculi to fluid shear stresses (23, 28, 29, 44). In a parallel plate flow chamber, an increase in chemotransport is predicted only between 0 and 0.25 dyn/cm^2 (3). Dose-dependent shear stress, release of NO, and shear-induced increases of intracellular calcium have been demonstrated to be independent of chemotransport (14, 22, 34). Therefore, it is unlikely that chemotransport mediates flow-induced signaling at shear above 0.25 dyn/cm^2. Similarly, streaming potentials are also dependent on shear rate but do not vary with viscosity (22). Although other possible signaling mechanisms of shear stress are not fully excluded, shear-induced signal transduction, independent of chemotransport or streaming potentials, likely represents the primary biophysical stimulus in the present study.

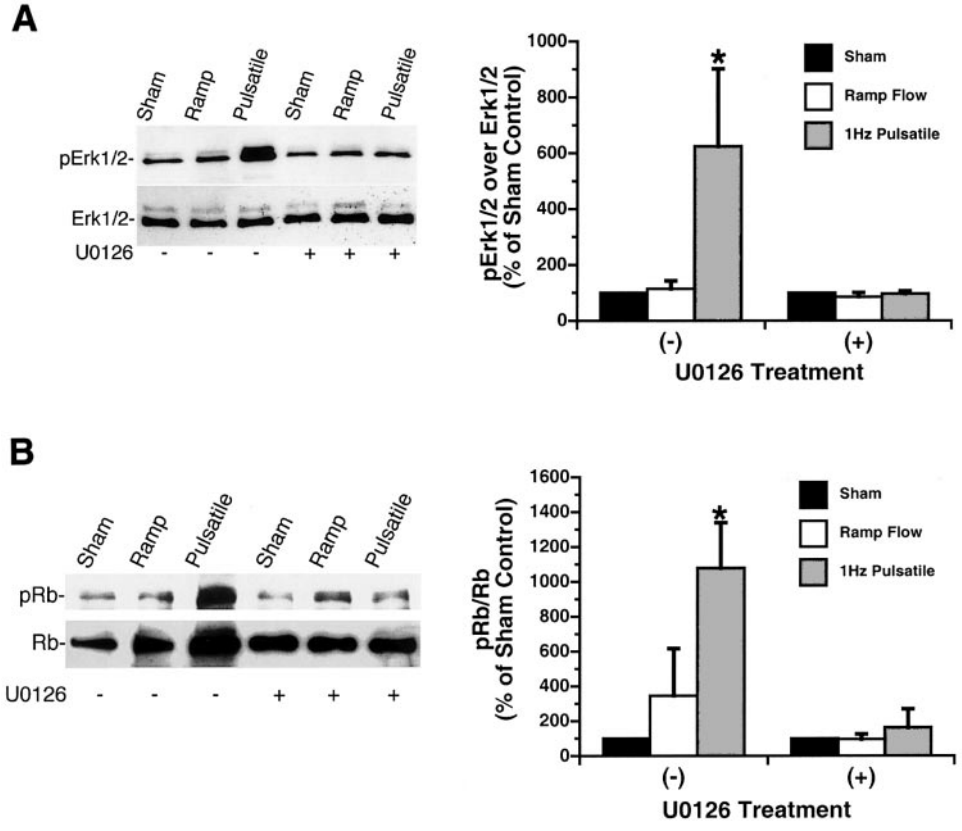

Fig. 5. U0126 abolished fluid flow-induced phosphorylation of ERK1/2 and Rb. *A*: Western blot showing the effect of U0126 treatment on phosphorylated ERK1/2 proteins (*left*). Densitometric quantification of flow-induced activation of ERK1/2. Relative levels of pERK1/2 over ERK1/2 (*right*). *B*: Western blot showing the effect of U0126 treatment on phosphorylated Rb proteins (*left*). Densitometric quantification of Rb phosphorylation. Relative levels of pRb over Rb (*right*). Values are expressed as means ± SD. *Significant increase compared with ramped steady flow ($P < 0.05$, $n = 3$).

In the present study, the mitogenic effect of fluid flow was assessed by BrdU incorporation (Fig. 1) and by changes in total cell number (Fig. 2). Under appropriate conditions, BrdU is substituted stoichiometrically for thymidine in newly replicated DNA in a time-related and concentration-dependent manner. Once a cell has entered S phase (which in this case is marked by the uptake of BrdU), it is generally considered to be fully committed to replication. To segregate cells directly stimulated by flow from the subsequent replication of daughter cells under static conditions, BrdU incorporation was assessed 1.5 h after cells had been exposed to flow. In relatively slow-growing rat primary osteoblastic cells, BrdU incorporation was also assessed at 24 h. When exposed to pulsatile flow, several BrdU-negative cells were observed in the later stages of telophase (arrows in Fig. 1*A*), indicating that these cells had completed DNA synthesis before BrdU labeling. This phenomenon suggests that pulsatile fluid flow may be able to promote mitosis and facilitate G2/M phase transition. ERK1/2 activation has been reported to regulate G2/M transition and mitotic exit (M/G1 transition) (9, 49). Activation of ERK1/2 promotes the completion of cell division within 80 min (48). In contrast, the abolishment of ERK1/2 activation induces a prompt G2 arrest in synchronized G1/S cells (9, 49). This may also explain why cell number increased following pulsatile flow after only 1.5 h (Fig. 2).

Phosphorylation of Rb controls the cell cycle transition from G1 phase to S phase. Rb phosphorylation causes the release of the E2F transcription factor, which is committed to promote the entrance of S phase from G1 (6). The phosphorylation of Rb is regulated by cyclin-dependent kinases (CDK) in combination with cyclin D_1 (1). The induction of cyclin D_1 transcription can be activated by the MAPK-signaling pathway (1, 5, 7). ERK1/2 activation is regulated by the upstream enzyme MEK1/2. ERK1/2 activation can be specifically blocked by the MEK1/2 inhibitor U0126. In the present study, U0126 was able to block the activation of ERK1/2 induced by temporal gradients in shear (Fig. 5*A*). U0126 also abolished the phosphorylated form of Rb resulting from the stimulation of temporal gradients in shear (Fig. 5*B*). Subsequently, osteoblast proliferation stimulated by temporal gradients in shear was inhibited with the addition of ERK1/2 inhibitor (Figs. 1*B* and 2). These results suggest that the mitogenic effect of temporal gradients in shear may be mediated by the MAPK signal cascade. Upstream activation of ERK1/2 mediates Rb phosphorylation and cell cycle progression. Given that the MAPK pathway is involved in the upregulation of the transcription of cyclin D_1, which forms a complex with CDK4 to phosphorylate Rb, it follows that the activity of ERK1/2 regulates Rb phosphorylation. Although Rb phosphorylation was not significantly elevated above sham controls in response to ramp flow (Fig. 5*B*), it should be noted that pRb was enhanced at 1.5 h. This is consistent with the finding that ramp flow also resulted in a nonsignificant elevation of pERK1/2 at an earlier time point (Fig. 4*B*). It is possible that the transient elevation of pERK1/2 also led to a similar downstream response in pRb.

In summary, we have shown that temporal gradients in shear stress lead to enhanced osteoblast proliferation in both transformed osteoblast-like UMR106 cells and primary osteoblastic cells, whereas steady, uniform shear stress affects proliferation no differently than in sham controls. Furthermore, the promitogenic stimulus of the temporal gradient was linked to the ERK1/2-signaling pathway and the subsequent phosphorylation of Rb. Thus this study suggests that cultured bone cells are more responsive to unsteady fluid shear stress, which in vivo may stimulate proliferation of osteoblasts in response to changes in mechanical loading.

We thank Susan Toyama for valuable assistance.

This study was supported by National Aeronautics and Space Administration Grants NAG8-1589 and NAG5-4648 and National Heart, Lung, and Blood Institute Grant HL-40696.

REFERENCES

1. **Albanese C, Johnson J, Watanabe G, Eklund N, Vu D, Arnold A, and Pestell RG.** Transforming p21ras mutants and c-Ets-2 activate the cyclin D1 promoter through distinguishable regions. *J Biol Chem* 270: 23589–23597, 1995.
2. **Bao X, Clark CB, and Frangos JA.** Temporal gradient in shear-induced signaling pathway: involvement of MAP kinase, c-fos and connexin-43. *Am J Physiol Heart Circ Physiol* 278: H1598–H1605, 2000.
3. **Berthiaume F.** Model of flow-induced convection of ATP. In: *Mechanism of Flow-Induced Stimulation of Endothelial Cells* (PhD thesis). Pennsylvania State University, 1992, p. 134–138.
4. **Cobb MH, Boulton TG, and Robbins DJ.** Extracellular signal-regulated kinases: ERKs in progress. *Cell Regul* 12: 965–978. 1991.
5. **Fribourg AF, Knudsen KE, Strobeck MW, Lindhorst CM, and Knudsen ES.** Differential requirements for Ras and the retinoblastoma tumor suppressor protein in the androgen dependence of prostatic adenocarcinoma cells. *Cell Growth Differ* 11: 361–372, 2000.
6. **Fry DW, Harvey PH, Bedford DC, Fritsch A, Keller PR, Wu Z, Dobrusin E, Leopold WR, Fattaey A, and Garrett MD.** Cell cycle and biochemical effects of PD0183812: a potent inhibitor of the cyclin D-dependent kinases CDK4 and CDK6. *J Biol Chem* 276: 16617–16623, 2001.
7. **Gille H and Downward J.** Multiple ras effector pathways contribute to G(1) cell cycle progression. *J Biol Chem* 274: 22033–22040, 1999.
8. **Haidekker MA, White CR, and Frangos JA.** Analysis of temporal shear stress gradients during the onset phase of flow over a backward-facing step. *J Biomech Eng* 123: 455–463, 2001.
9. **Hayne C, Tzivion G, and Luo Z.** Raf-1/MEK/MAPK pathway is necessary for the G2/M transition induced by nocodazole. *J Biol Chem* 275: 31876–31882, 2000.
10. **Hillsley MV and Frangos JA.** Bone tissue engineering: the role of interstitial fluid flow. *Biotechnol Bioeng* 43: 573–581, 1994.
11. **Hillsley MV and Frangos JA.** Alkaline phosphatase in osteoblasts is down-regulated by pulsatile fluid flow. *Calcif Tissue Int* 60: 48–53, 1997.
12. **Hu YL, Li S, Shyy JY, and Chien S.** Sustained JNK activation induces endothelial apoptosis: studies with colchicine and shear stress. *Am J Physiol Heart Circ Physiol* 277: H1593–H1599, 1999.
13. **Hung CT, Pollack SR, Reilly TM, and Brighton CT.** Real-time calcium response of cultured bone cells to fluid flow. *Clin Orthop* 313: 256–269, 1995.
14. **Hung CT, Allen FD, Pollack SR, and Brighton CT.** What is the role of the convective current density in the real-time cal-

cium response of cultured bone cells to fluid flow? *J Biomech* 29: 1403–1409, 1996.
15. **Hunter T and Karin M.** The regulation of transcription by phosphorylation. *Cell* 70: 375–387, 1992.
16. **Jacobs CR, Yellowley CE, Davis BR, Zhou Z, Cimbala JM, and Donahue HJ.** Differential effect of steady versus oscillating flow on bone cells. *J Biomech* 31: 969–976, 1998.
17. **Johnson DL, McAllister TN, and Frangos JA.** Fluid flow stimulates rapid and continuous release of nitric oxide in osteoblasts. *Am J Physiol Endocrinol Metab* 271: E205–E208, 1996.
18. **Johnson GL and Vaillancourt RR.** Sequential protein kinase reactions controlling cell growth and differentiation. *Curr Opin Cell Biol* 6: 230–238, 1994.
19. **Karin M and Hunter T.** Transcriptional control by protein phosphorylation: signal transmission from the cell surface to the nucleus. *Curr Biol* 5: 747–757, 1995.
20. **Kortylewski M, Heinrich PC, Kauffmann ME, Bohm M, MacKiewicz A, and Behrmann I.** Mitogen-activated protein kinases control p27/Kip1 expression and growth of human melanoma cells. *Biochem J* 357: 297–303, 2001.
21. **Mak AFT, Qin L, Hung LK, Cheng CW, and Tin CF.** A histomorphometric observation of flows in cortical bone under dynamic loading. *Microvasc Res* 59: 290–300, 2000.
22. **McAllister TN and Frangos JA.** Steady and transient fluid shear stress stimulate NO release in osteoblasts through distinct biochemical pathways. *J Bone Miner Res* 14: 930–936, 1999.
23. **Montgomery RJ, Sutker BD, Bronk JT, Smith SR, and Kelly PJ.** Interstitial fluid flow in cortical bone. *Microvasc Res* 35: 295–307, 1988.
24. **Nillson BE.** Bone density in athletes. *Clin Orthop Rel Res* 77: 179–182, 1971.
25. **Noble B, Routledge J, Stevens H, Hughes I, and Jacobsen W.** Androgen receptors in bone-forming tissue. *Horm Res* 51: 31–36, 1999.
26. **Ono K and Han J.** The p38 signal transduction pathway: activation and function. *Cell Signal* 12: 1–13, 2000.
27. **Osada S, Saji S, and Osada K.** Critical role of extracellular signal-regulated kinase phosphorylation on menadione (vitamin K3) induced growth inhibition. *Cancer* 91: 1156–1165, 2001.
28. **Otter MW, Palmieri VR, and Cochran GV.** Transcortical streaming potentials are generated by circulatory pressure gradients in living canine tibia. *J Orthop Res* 8: 119–126, 1990.
29. **Piekarski K and Munro M.** Transport mechanism operating between blood supply and osteocytes in long bones. *Nature* 269: 80–82, 1977.
30. **Qin YX, McLeod KJ, and Rubin CT.** Intracortical fluid flow is induced by dynamic intramedullary pressure independent of matrix deformation (Abstract). *Trans Ortho Res Soc* 25: 740, 2000.
31. **Reich KM, Gay CV, and Frangos JA.** Fluid shear stress as a mediator of osteoblast cyclic adenosine monophosphate production. *J Cell Physiol* 143: 100–104, 1990.
32. **Reich KM and Frangos JA.** Effect of flow on prostaglandin E_2 and inositol trisphosphate levels in osteoblasts. *Am J Physiol Cell Physiol* 261: C428–C432, 1991.
33. **Reich KM and Frangos JA.** Protein kinase C mediates flow-induced prostaglandin E_2 production in osteoblasts. *Calcif Tissue Int* 52: 62–66, 1993.
34. **Reich KM.** *Fluid Flow-Induced Signal Transduction in Osteoblasts* (PhD thesis). Pennsylvania State University, 1993.
35. **Reich KM, McAllister TN, Gudi S, and Frangos JA.** Activation of G proteins mediates flow-induced prostaglandin E2 production in osteoblasts. *Endocrinology* 138: 1014–1018, 1997.
36. **Roer RD and Dillaman RM.** Bone growth and calcium balance during simulated weightlessness in the rat. *J Appl Physiol* 68: 13–20, 1990.
37. **Shan B, Durfee T, and Lee WH.** Disruption of RB/E2F-1 interaction by single point mutations in E2F-1 enhances S-phase entry and apoptosis. *Proc Natl Acad Sci USA* 93: 679–684, 1996.
38. **Stanford CM, Jacobsen PA, Eanes ED, Lembke LA, and Midura RJ.** Rapidly forming apatitic mineral in an osteoblastic cell line (UMR 106–01 BSP). *J Biol Chem* 270: 9420–9428, 1995.
39. **Steck R, Niederer P, and Knothe Tate ML.** A finite difference model of load-induced fluid displacements within bone under mechanical loading. *Med Eng Phys* 22: 117–125, 2000.
40. **Stringa E, Filanti C, Giunciuglio D, Albini A, and Manduca P.** Osteoblastic cells from rat long bone. I. Characterization of their differentiation in culture. *Bone* 16: 663–670, 1995.
41. **Stevens HY, Reeve J, and Noble BS.** Bcl-2, tissue transglutaminase and p53 protein expression in the apoptotic cascade in ribs of premature infants. *J Anat* 196: 181–191, 2000.
42. **Srinivasan S and Gross TS.** Canalicular fluid flow induced by bending of a long bone. *Med Eng Phys* 22: 127–133, 2000.
43. **Tavassoli M and Yoffey JM.** *Bone Marrow Structure and Function* (1st ed.). New York: Liss, 1983, p. 65–83.
44. **Weinbaum S, Cowin SC, and Zeng YA.** A model for the excitation of osteocytes by mechanical loading induced bone fluid shear stresses. *J Biomech* 27: 339–360, 1994.
45. **Whedon GD.** Disuse osteoporosis: physiological aspects. *Calcif Tissue Int* 36, *Suppl* 1: S146–S150, 1984.
46. **White CR, Haidekker M, Bao X, and Frangos JA.** Temporal gradients in shear, but not spatial gradients, stimulate endothelial cell proliferation. *Circulation* 103: 2508–2513, 2001.
47. **Widmann C, Gibson S, Jarpe MB, and Johnson GL.** Mitogen-activated protein kinase: conservation of a three-kinase module from yeast to human. *Physiol Rev* 79: 143–180, 1999.
48. **Willard FS and Crouch MF.** MEK, ERK, and p90RSK are present on mitotic tubulin in Swiss 3T3 cells: a role for the MAP kinase pathway in regulating mitotic exit. *Cell Signal* 13: 653–664, 2001.
49. **Wright JH, Munar E, Jameson DR, Andreassen PR, Margolis RL, Seger R, and Krebs EG.** Mitogen-activated protein kinase kinase activity is required for the G(2)/M transition of the cell cycle in mammalian fibroblasts. *Proc Natl Acad Sci USA* 96: 11335–11340, 1999.